NASA/CR—2000-209309

Development and Characterization of Laser-Induced Incandescence Towards Nanoparticle (Soot) Detection

Randy L. Vander Wal
National Center for Microgravity Research, Cleveland, Ohio

February 2000

The NASA STI Program Office . . . in Profile

Since its founding, NASA has been dedicated to the advancement of aeronautics and space science. The NASA Scientific and Technical Information (STI) Program Office plays a key part in helping NASA maintain this important role.

The NASA STI Program Office is operated by Langley Research Center, the Lead Center for NASA's scientific and technical information. The NASA STI Program Office provides access to the NASA STI Database, the largest collection of aeronautical and space science STI in the world. The Program Office is also NASA's institutional mechanism for disseminating the results of its research and development activities. These results are published by NASA in the NASA STI Report Series, which includes the following report types:

- TECHNICAL PUBLICATION. Reports of completed research or a major significant phase of research that present the results of NASA programs and include extensive data or theoretical analysis. Includes compilations of significant scientific and technical data and information deemed to be of continuing reference value. NASA's counterpart of peer-reviewed formal professional papers but has less stringent limitations on manuscript length and extent of graphic presentations.

- TECHNICAL MEMORANDUM. Scientific and technical findings that are preliminary or of specialized interest, e.g., quick release reports, working papers, and bibliographies that contain minimal annotation. Does not contain extensive analysis.

- CONTRACTOR REPORT. Scientific and technical findings by NASA-sponsored contractors and grantees.

- CONFERENCE PUBLICATION. Collected papers from scientific and technical conferences, symposia, seminars, or other meetings sponsored or cosponsored by NASA.

- SPECIAL PUBLICATION. Scientific, technical, or historical information from NASA programs, projects, and missions, often concerned with subjects having substantial public interest.

- TECHNICAL TRANSLATION. English-language translations of foreign scientific and technical material pertinent to NASA's mission.

Specialized services that complement the STI Program Office's diverse offerings include creating custom thesauri, building customized data bases, organizing and publishing research results . . . even providing videos.

For more information about the NASA STI Program Office, see the following:

- Access the NASA STI Program Home Page at ***http://www.sti.nasa.gov***

- E-mail your question via the Internet to help@sti.nasa.gov

- Fax your question to the NASA Access Help Desk at (301) 621-0134

- Telephone the NASA Access Help Desk at (301) 621-0390

- Write to:
  NASA Access Help Desk
  NASA Center for AeroSpace Information
  7121 Standard Drive
  Hanover, MD 21076

NASA/CR—2000-209309

Development and Characterization of Laser-Induced Incandescence Towards Nanoparticle (Soot) Detection

Randy L. Vander Wal
National Center for Microgravity Research, Cleveland, Ohio

Prepared for the
Symposium on Nanoparticles
cosponsored by the National Science Foundation and the European Science Foundation
Tacoma, Washington, October 10, 1999

Prepared under Cooperative Agreement NAS3–544

National Aeronautics and
Space Administration

Glenn Research Center

February 2000

Acknowledgments

This work was supported through NASA contract NAS3–27186 with Nyma Inc. and presently through NASA cooperative agreement NAS3–544 with the National Center for Microgravity Research on Fluids and Combustion.

Available from

NASA Center for Aerospace Information
7121 Standard Drive
Hanover, MD 21076
Price Code: A03

National Technical Information Service
5285 Port Royal Road
Springfield, VA 22100
Price Code: A03

Development and Characterization of Laser-Induced Incandescence Towards Nanoparticle (Soot) Detection

Dr. Randy L. Vander Wal
National Center for Microgravity Research on Fluids and Combustion
National Aeronautics and Space Administration
Glenn Research Center
Cleveland, Ohio 44135

Motivation

The production of particulates, notably soot, during combustion has both positive and negative ramifications. Exhaust from diesel engines under load (for example, shifting gears), flickering candle flames and fireplaces all produce soot leaving a flame. From an efficiency standpoint, emission of soot from engines, furnaces or even a simple flickering candle flame represents a loss of useful energy.

The emission of soot from diesel engines, furnaces, power generation facilities, incinerators and even simple flames poses a serious environmental problem and health risk [1]. Yet some industries intentionally produce soot as carbon black for use in inks, copier toner, tires and as pigments. Similarly, the presence of soot within flames can act both positively and negatively. Energy transfer from a combustion process is greatly facilitated by the radiative heat transfer from soot yet radiative heat transfer also facilitates the spread of unwanted fires. To understand soot formation and develop control strategies for soot emission/formation, measurements of soot concentration in both practical devices such as engines and controlled laboratory flames are necessary. Laser-induced incandescence (LII) has been developed and characterized to address this need, as described here.

Background

The phenomena of incandescence can be used as a diagnostic to determine soot concentration or soot volume fraction (defined as the volume of soot per unit volume of space, a dimensionless quantity). When pulsed high intensity laser light heats soot far above flame temperature, the soot will incandesce strongly throughout the visible region of the spectrum. The fact that pulsed high intensity laser light can elevate the soot particle temperature even when the soot glows in flames was observed long ago but considered an interference in pulsed laser diagnostics [2]. Only recently have researchers demonstrated that this laser-induced emission can be used as a measure of the soot concentration [3-7], thereby validating theoretical predictions [8-12]. In accord with the Planck radiation law, soot's radiative emission at these elevated temperatures increases in intensity and shifts to blue wavelengths as compared with the non-laser-heated soot and flame gases [13]. Because it is pulsed and blue shifted, the LII signal is readily isolated from natural flame emission.

Alternative methods of measuring soot volume fraction include physical sampling of the soot and measuring the absorption caused by soot. Sampling lacks high temporal and spatial resolution and requires an intrusive probe that can perturb the combustion process. Absorption lacks high temporal resolution, can be complicated by scattering, requires knowledge of the path

length and makes assumptions regarding soot physical properties. In contrast, LII offers high spatial and temporal resolution and can be used for multidimensional measurements [4-7,14-17]. Additionally, LII provides a measure of the soot volume fraction nearly independent of contributions from both scattering by soot aggregates and absorption by polycyclic aromatic hydrocarbons.

In addition to its application to steady-state systems, such as laminar gas-jet diffusion flames, LII is also ideally suited to measuring soot concentrations in phenomena with rapid time-scales lacking spatial symmetry such as turbulent combustion processes [5,18]. This is possible because measurements may be obtained from a single laser pulse in detection times as short as 10 ns. Since LII is not a line-of-sight technique, it also possesses geometric versatility enabling its application to nonaxisymmetric systems. Examples demonstrating the capabilities of LII will be given during the presentation.

Experimental Details

Figure 1 is an experimental schematic which illustrates typical experimental hardware. For incandescence measurements, a pulsed laser source, beam delivery and signal collection optics, and detector are necessary. For point measurements, a photomultiplier is adequate while imaging measurements require a gated intensified array camera. Timing electronics synchronizing the laser and data acquisition are necessary. Either detector is usually preceded by a wavelength filter such as a bandpass interference filter or spectrograph.

Characterization of Laser-induced incandescence as a Diagnostic Technique

The implementation of LII, as a diagnostic technique, requires attention to excitation and detection conditions. Excitation conditions include excitation laser wavelength and fluence. Detection conditions include the time for initial signal detection, the duration of signal collection and the spectral region comprising the detected signal.

Excitation Wavelength

High intensity ultraviolet laser pulses are known to produce unwanted photochemical processes in soot containing flames. Examples of undesirable emission include fluorescence from aromatic species and photofragment fluorescence which are readily generated by wavelengths associated with excimer lasers and harmonics of Nd:YAG lasers. The prompt occurrence of these laser-induced emission processes can compete with laser-induced incandescence of soot thereby adding a spurious signal that will likely be unrelated to the soot concentration. While delayed detection can remove these unwanted emission contributions through collisional quenching of the fluorescence, inaccuracies in the LII measurement can then arise due to particle size-dependent cooling processes [9-12,16,19,20]. Thus the choice of excitation wavelength is mainly determined by avoiding the creation of these photochemical interferences.

The near infrared wavelength of 1064 nm, the fundamental of the Nd:YAG laser, has proven advantages in the generation of LII [4,21,22]. In general it is energetically incapable of causing the aforementioned fluorescence processes except via multiphoton absorption. Such IR multiphoton absorption is unlikely given the absence of molecular resonances at 1064 nm. Even if IR multiphoton absorption did result in molecular decomposition, it would produce molecular fragments in the ground electronic state.

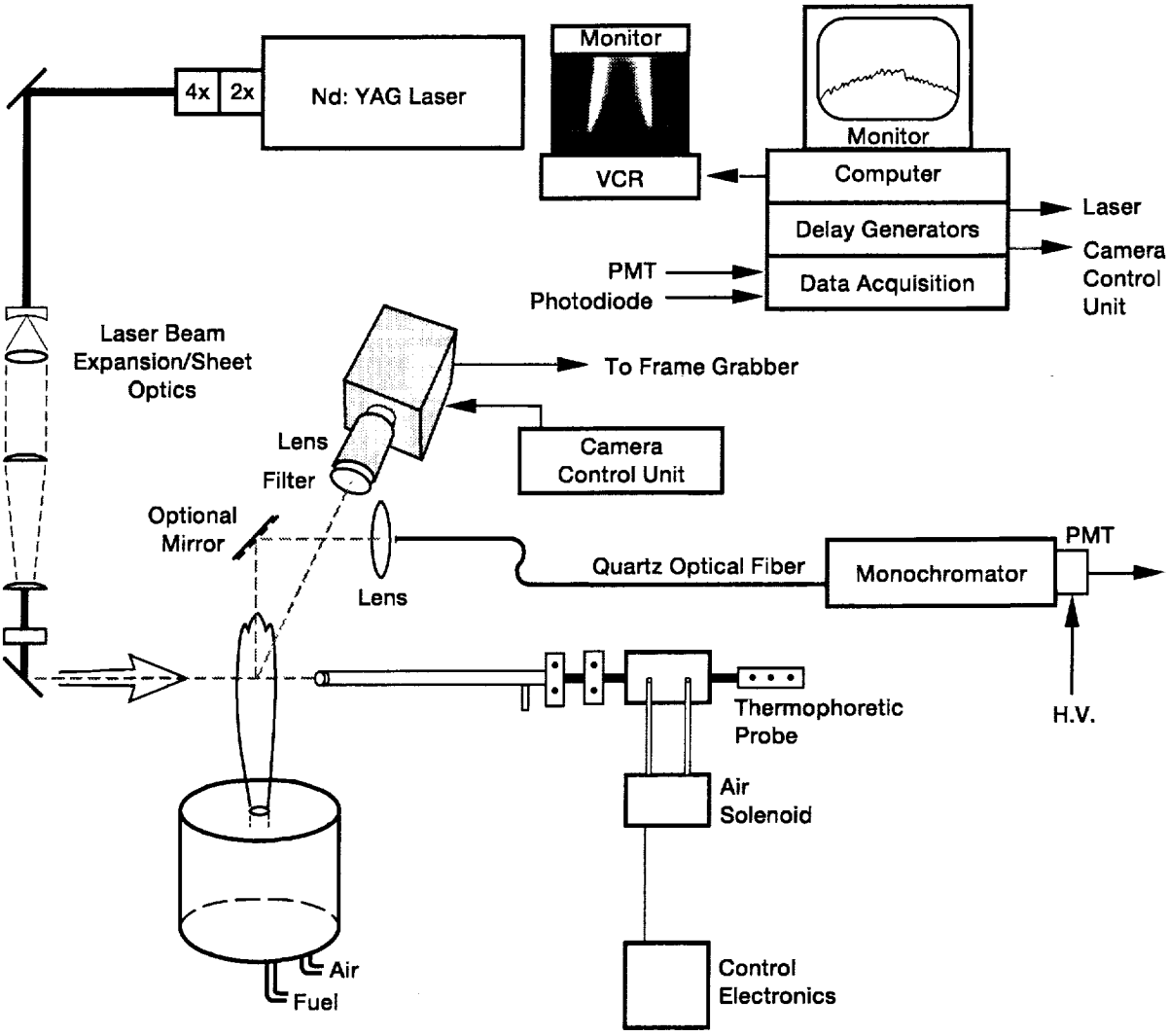

Figure 1.—Experimental Schematic.

Excitation Laser Fluence

Laser fluence is a relevant parameter when heating Rayleigh-size particles with nanosecond duration laser pulses. The appropriate laser fluence has been a more difficult parameter to specify for LII than excitation wavelength. Initial measurements developed fluence dependence curves relating the LII signal intensity to the laser fluence. Essentially two types of patterns were observed. One result was a curve with different multiple slopes but which continued to increase with increasing laser fluence [5,17]. The other fluence dependence behavior observed was a strong initial increase in signal with fluence followed by a plateau region where the signal was relatively independent of the laser fluence [4,16,21,22]. This region was then followed by a decrease in signal with further increases in laser fluence. The decrease was interpreted as representing mass loss from the incandescing particles due to laser vaporization. The current consensus is that these observed patterns were in part created by laser-beam wing-effects which cause larger volumes of soot to be heated to incandescent temperatures with increasing laser fluence. This effect can offset signal decreases due to vaporization-induced mass depending on detection geometry.

An example of the variation of LII intensity with laser fluence is shown in Fig. 2. Radial LII intensity profiles are shown that were generated within a laminar ethylene gas-jet diffusion flame. Shown are profiles generated by an initial laser pulse and a second laser pulse, delayed from the first by 50 μsec. This delay allows the soot heated by the first pulse to cool to local flame temperature while allowing the second laser pulse to reheat the same soot as was heated by the first laser pulse. Although a range of LII intensities are produced by each laser pulse, those generated by the second laser pulse are in general markedly lower than those generated by the first laser pulse for equal fluence values, particularly at high values of laser fluence. These changes are interpreted as resulting from a combination of laser-induced morphological changes for fluences below 0.5 J/cm^2 and additional laser-induced vaporization mass loss at higher laser fluences. Normalization of the profiles by their radially-integrated intensity reveals that the profiles are self-similar at the axial positions of 60 and 20 mm HAB, as shown in Fig. 3, even those produced by the second laser pulse! Differences are observed at 40 mm HAB. Notably, these differences in LII intensity for each laser pulse and between the two pulses (for equal fluence values) become greater with increasing laser fluence.

The differences between the unnormalized intensity profiles produced by the two laser pulses indicates that significant changes are introduced by the pulsed high intensity laser light. That normalization can lead to self-similarity indicates that the soot properties and subsequent changes are uniform in spatial position, such as at 60 mm HAB. Radial differences in soot size and composition lead to the observed radial differences at the axial position of 40 mm HAB. Thus the accuracy of comparison of LII intensities at different spatial locations in a given system will depend upon the uniformity of the soot at these positions and the value of the laser fluence. Thus the suitable laser fluence will likely depend upon the application.

Calibration

LII is a relative measurement technique that requires calibration for quantitative soot volume fraction determination. A corollary is that the accuracy of LII can never be greater than the accuracy of its calibration. Three sources of error can arise in the calibration of LII: (1) laser beam attentuation by soot absorption and vaporization, (2) LII signal attenuation by soot intervening between the measurement point/plane and detector and, most significantly, (3) the uncertainty in the value for the soot refractive index.

The need for calibration stems from the fact that existing theories describing LII include a number of assumptions regarding the physical and optical properties of the soot at the elevated temperatures corresponding to visible incandescence [2,9-12]. In addition, these theories assume that soot primary particles are point-contacting, noninteracting spherules within aggregates and that no physical or chemical changes occur in the laser heated soot. TEM micrographs of soot collected from various flames reveal highly connected primary particles. Thermophoretic sampling of laser-heated soot has shown that graphitization of the soot occurs with the extent of graphitization depending upon the laser fluence [23]. This is illustrated in Fig. 4.

Additional uncertainties include the formulation of the heat conduction to the local ambient environment which governs the cooling of the laser heated soot (shortly after the laser pulse) and the influence of aggregate structure upon the cooling rate. Recently an alternative theoretical formalism describing LII has been developed by Filippov et al., [24]. This theory

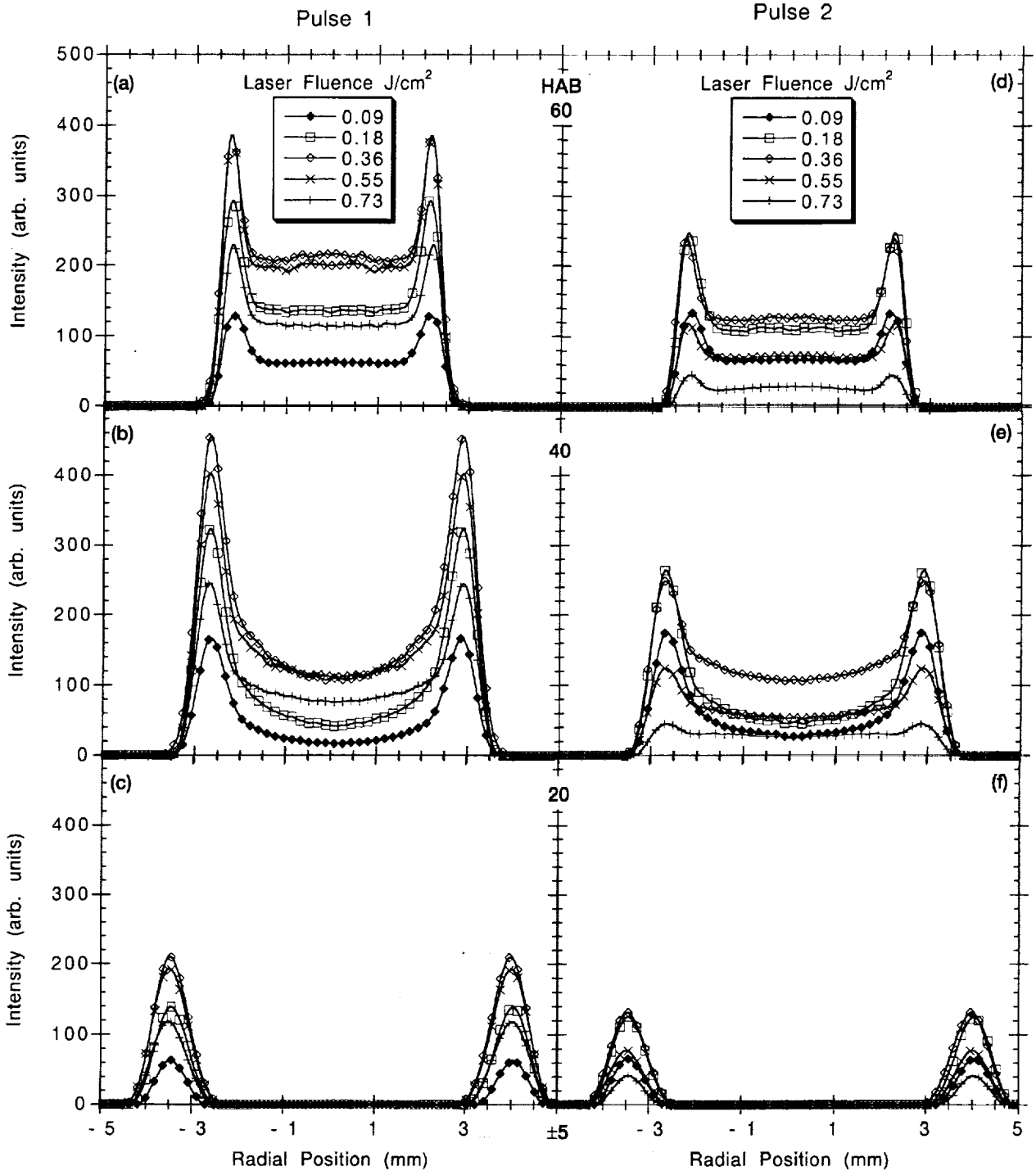

Figure 2.—Radial LII intensity profiles obtained at the indicated heights above the burner (HAB).

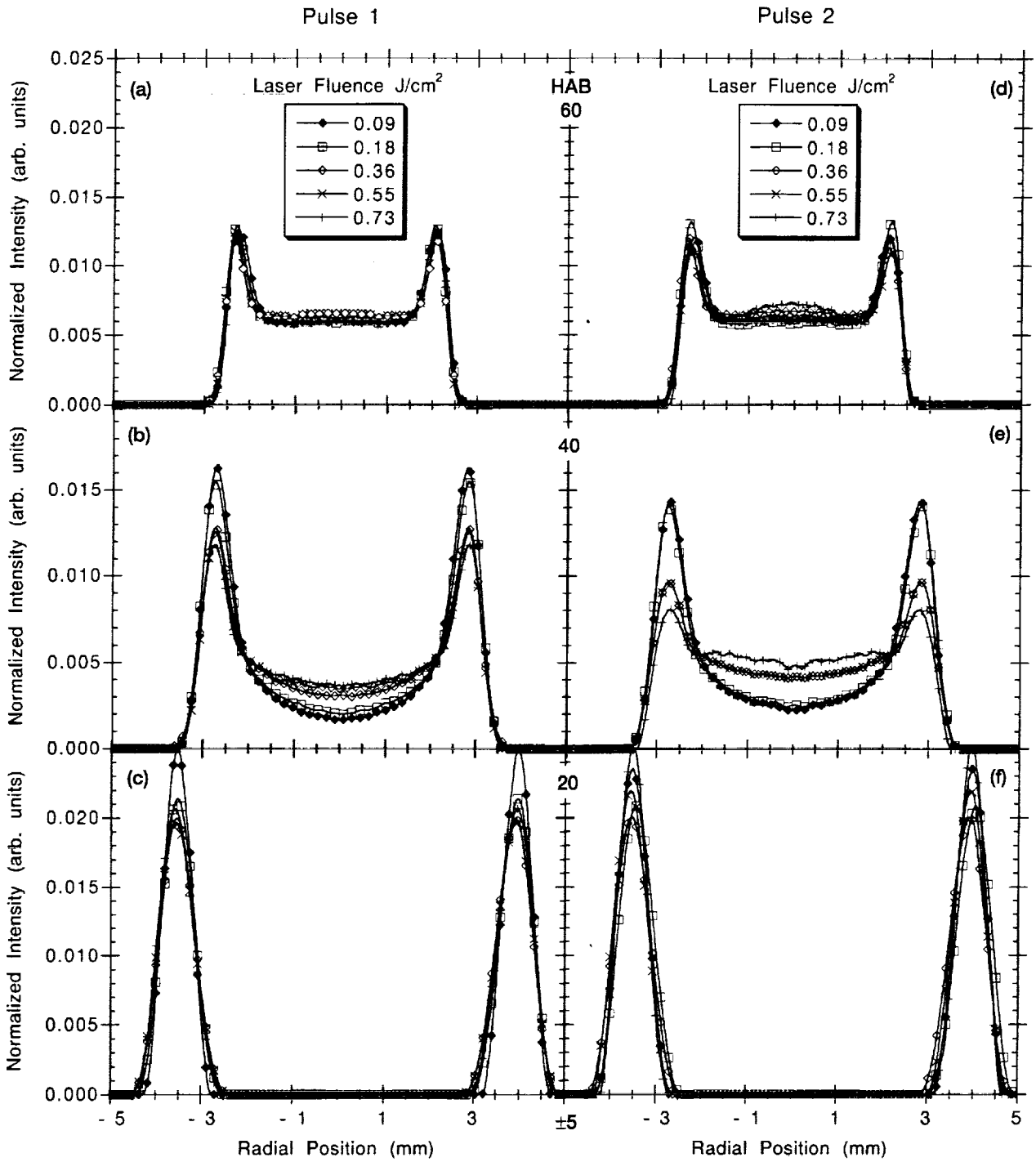

Figure 3.—Normalized radial LII intensity profiles from Figure 2.

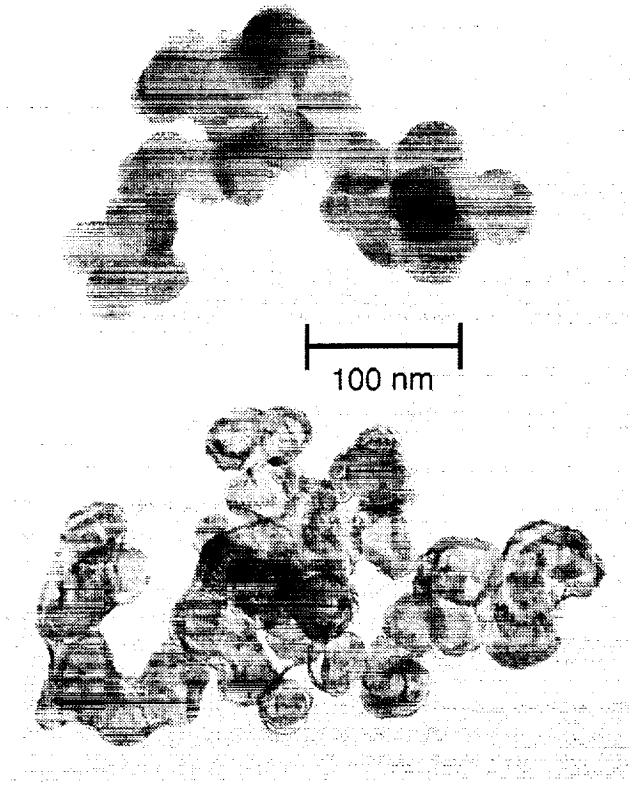

Figure 4.—Transmission Electron Microscopy images of a representative soot aggregate (top) and a soot aggregate subjected to pulsed laser heating (bottom).

yields a Fredholm integral equation describing the temporal variation of the LII signal and its dependence upon nanoparticle physical properties and aggregate size effects. It has already been proven to accurately capture the heat transfer occurring through conduction from the laser heated soot [25]. With its inclusive formalism, this model is potentially capable of yielding both primary particle and soot aggregate size. Further experimental testing is expected.

Detection Wavelength

The detection wavelength constitutes another variable in LII for which many choices are appropriate. The overriding consideration is that the specific detected wavelength not coincide with photofragment fluorescence or other spectral interferences (laser-induced or otherwise) associated with the combustion process. In addition, the detected wavelength interval should be sufficiently large to provide adequate signal while the wavelengths collected should minimize flame luminosity as a background source. This is readily accomplished by detection of incandescence in the near ultraviolet. It should be noted that according to the theory developed by Melton and Eckbreth [2,9], longer detection wavelengths yield a truer measure of the soot volume fraction. From an experimental standpoint, long wavelength detection does provide significantly larger signals and greater immunity to particle size dependent cooling processes yet it does not offer as much spectral discrimination against natural flame luminosity as ultraviolet detection.

Detection Time

The most accurate soot volume fraction measurements are obtained by signal collection during the peak of the laser pulse where the soot particles are at their maximum temperature [5,12,17,20-23]. Physically, this is consistent with minimizing particle size dependent cooling processes that will become dominated by the particle surface area for cooling by conduction. Figure 5 shows radial intensity profiles for a selected set of measurement times and durations as indicated in the Figure. The profiles have been normalized by their respective peak intensities. As illustrated, the profiles remain similar for different detected wavelengths at the same detection time conditions. A comparison of radial intensity profiles for various collection gates shows that gates that are prompt, beginning with the peak of the LII signal, yield a more similar radial profile than those beginning well after the excitation laser pulse. Those gates that are shorter in duration (compare gates 2 & 5; 3 & 4) yield radial profiles closer to that obtained using gate type 1. These differences are readily interpretable in terms of primary particle size and local temperature. Soot particles near the flame centerline cool faster due to their smaller primary particle size and the lower local ambient gas temperature at this axial height. Hence delayed detection or longer detection times accentuate the differences in primary particle size and local temperature.

Primary Particle Size Effects

This presentation has repeatedly emphasized that the LII signal is dependent upon primary particle size. Given this sensitivity, the potential exists for using LII as an optical technique for in-situ primary particle sizing. Two methods have been proposed based on theoretical calculations. These two approaches utilize a) the intensity ratio of the decaying LII signal at two different detected wavelengths at equal detection times or b) the temporal evolution of the signal at a single detected wavelength.

To test these approaches, we used different flames with different fuels to produce primary particles of different size yet at similar temperatures [20]. The temporal evolution of the LII signal generated by these different primary particles is illustrated in Fig. 6. A strong size dependence is observed. According to theory, the former approach, a), is predicted to be both monotonic and possess the stronger dependence upon particle size. As illustrated in Fig. 7 this is not realized in practice. The latter approach, b), does yield a monotonic relation between the LII decay rate and primary particle size as shown in Fig. 8. Using this method to develop a calibration database yielded good agreement with primary particle sizes directly measured from TEM micrographs in a laminar ethylene air diffusion flame within the early soot growth and late oxidation regions as seen in Fig. 9. The differences arise from aggregate size effects which can act to reduce the cooling rate of the primary particles [20].

Recent Advancements

We have recently characterized and demonstrated laser-induced incandescence for the measurement of metal nanoparticle concentrations [26]. A spectral and temporal survey of the laser-induced incandescence as a function of the excitation laser fluence and detection wavelength has been completed revealing new processes not previously observed in LII applied to soot. Validation of the incandescence as a measure of the concentration was demonstrated by absorption measurements. Fluence dependence measurements have also been made. Double pulse measurements were used to determine the fluence for the onset of vaporization-induced mass loss. Metals tested to-date include (in order of increasing vaporization temperature) Fe, Ti, Mo and W.

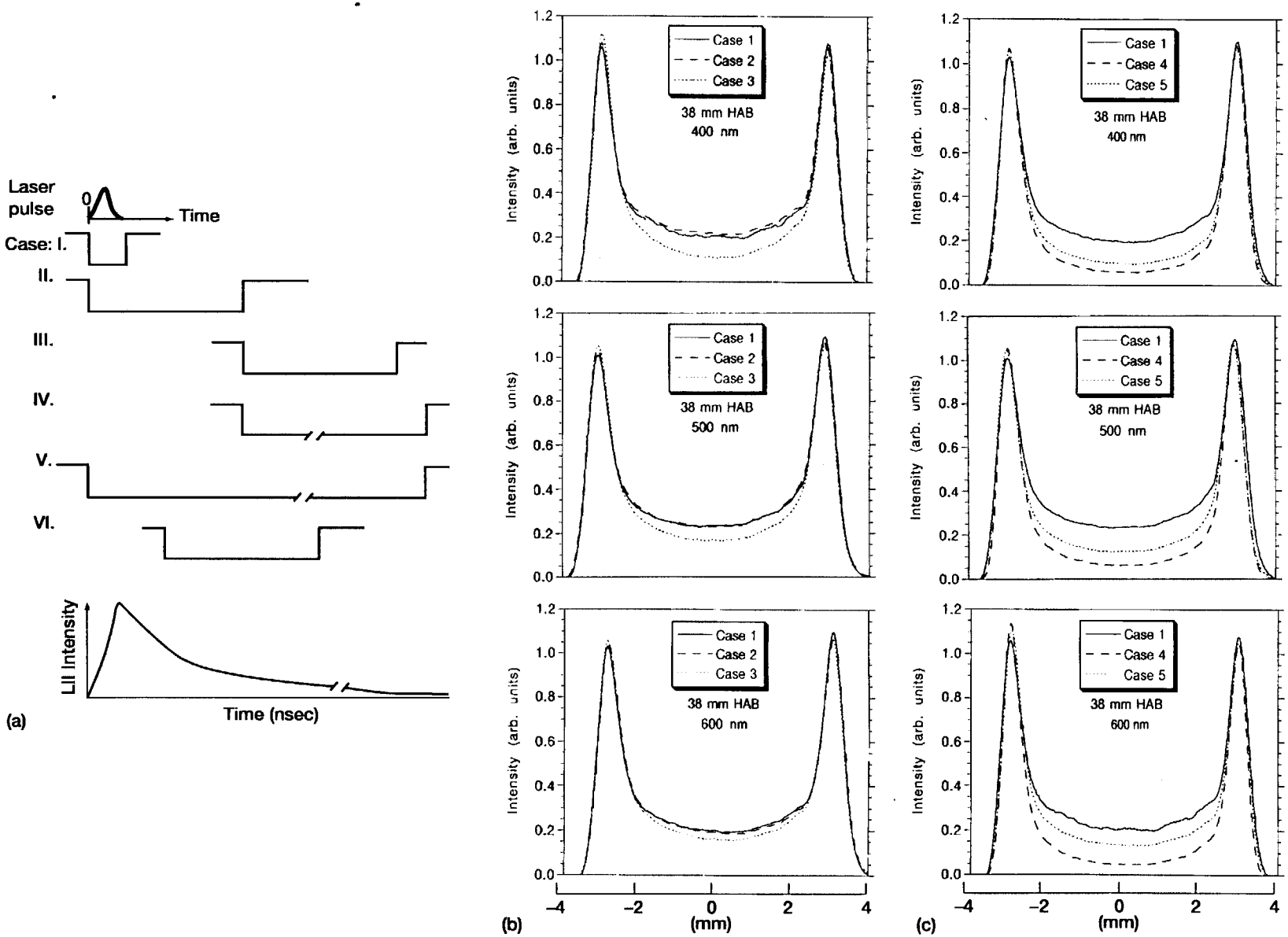

Figure 5.—(a) Timing chart of the LII signal collection strategies considered as cases 1-5. (b) Radial profiles of normalized LII intensity at 38 mm above the burner at the different indicated wavelengths where detection timing cases 1-3 are compared. (c) Radial profiles of normalized LII intensity at 38 mm above the burner at the different indicated wavelengths where detection timing cases 1, 4 , & 5 are compared.

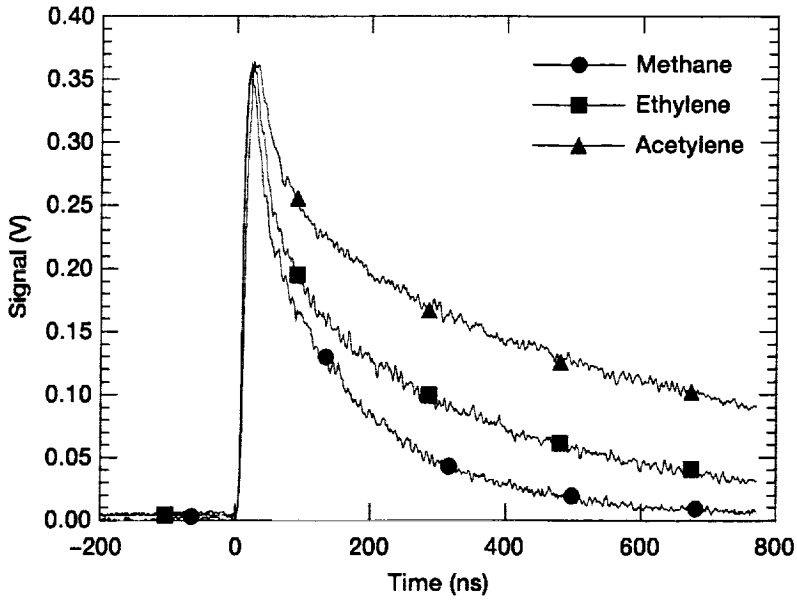

Figure 6.—Time-resolved LII signals produced by the different size primary particles produced by the diffusion flames of the different fuels.

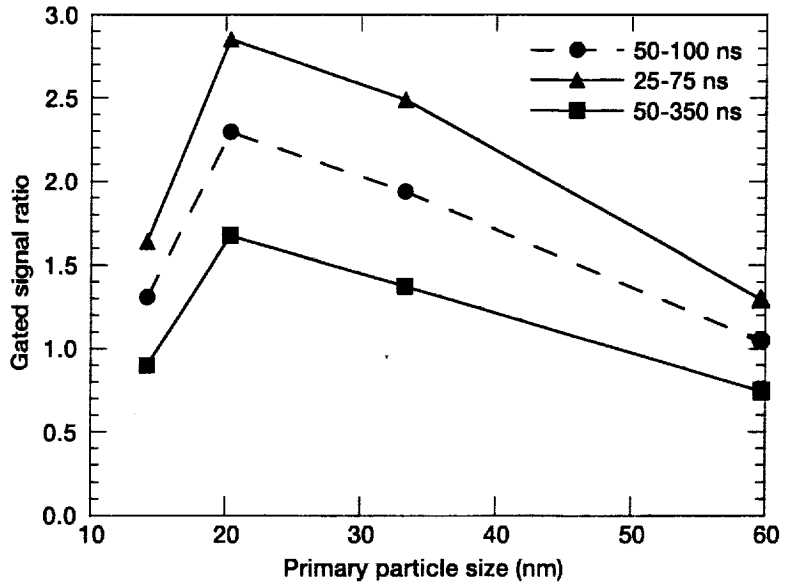

Figure 7.—Correlation between measured primary particle size and the signal intensity ratio between 300 nm and 600 nm for the different signal integration times. The points along each curve represent measurements (with increasing primary particle size) from methane, ethane, ethylene and acetylene respectively.

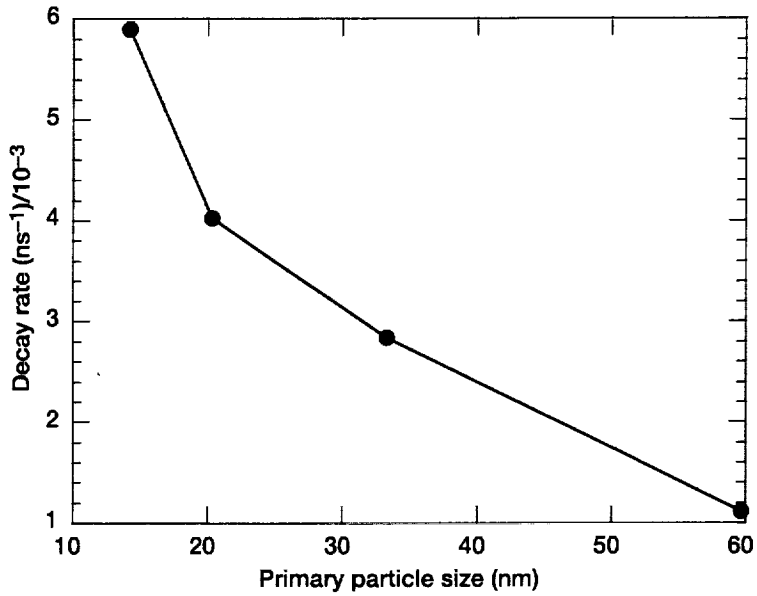

Figure 8.—Correlation between measured primary particle size and the second decay rate describing the temporally resolved LII signal. The points along each curve represent measurements (with increasing primary particle size) produced by the diffusion flames of methane, ethane, ethylene, and acetylene respectively.

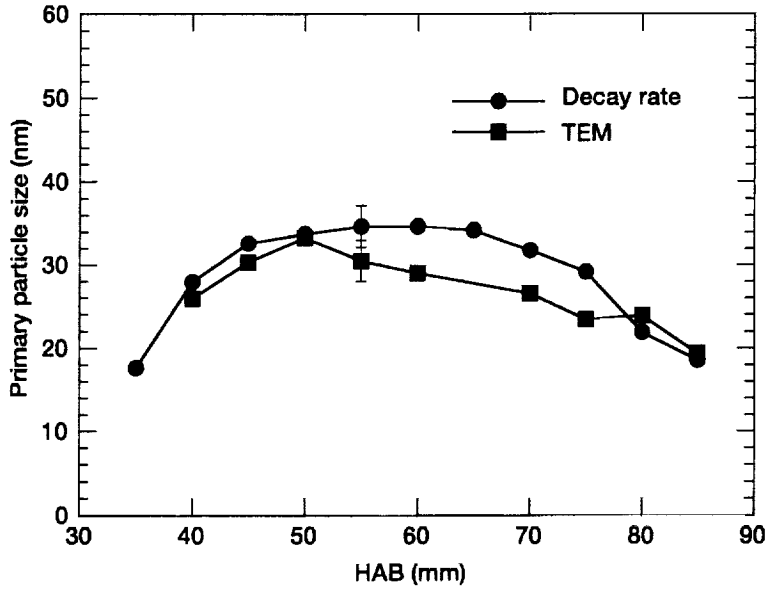

Figure 9.—Comparison between the predicted primary particle size based on the optical (LII) measurements and interpreted using the calibration curve in Fig. 8 and direct measurements from transmission electron microscopy micrographs.

References

1. Meyer, M.B., J. Aerosol Sci. 29, Suppl. 1, S713–S714 (1998).
2. Eckbreth, A.C., J. Appl. Phys. 48, 4473–4483 (1977).
3. Quay, B., Lee, T.W., Ni, T., and Santoro, R.J., Combust. and Flame 97, 394–395 (1994).
4. Vander Wal, R.L. and Weiland, K.J., Appl. Phys. B59, 445–452 (1994).
5. Tait, N.A. and Greenhalgh, D.A., Ber. Bunsenges Phys. Chem. 97, 1619–1625 (1993).
6. Shaddix, C.R., Harrington, J.E., and Smyth, K.C., Combust. and Flame, 99, 723–732 (1994).
7. Cignoli, F., Benecchi, S., and Zizak, G., Appl. Opt. 33, 5778–5782 (1994).
8. Pitz, R.W., Penney, C.M., Stanforth, C.M., and Shaffernocker, W.M., NASA CR–168287 (1984).
9. Melton, L.A., Appl. Opt. 23, 2201–2208 (1984).
10. Dasch, C.J., Appl. Opt. 23, 2209–2215 (1984).
11. Hofeldt, D.L., SAE Tech Paper 930079 (Society of Automotive Engineers, Warrendale, PA, 1993).
12. Mewes, B. and Seitzman, J.M., Appl. Opt. 36, 709–718 (1997).
13. Dec, J.E., zur Loye, A.O., and Siebers, D.L., SAE Tech. Paper 910224 (Society of Automotive Engineers, Warrensdale, PA, 1991).
14. Vander Wal, R.L., Twenty-Sixth Symposium (International) on Combustion, The Combustion Institute, Pittsburgh, PA, pp. 2269–2275 (1996).
15. Vander Wal, R.L., Combust. Sci. and Technol. 118, 343–360 (1996).
16. Ni, T., Pinson, J.A., Gupta, S., and Santoro, R.J., Appl. Opt. 34, 7083–7091 (1995).
17. Shaddix, C.R. and Smyth, K.C., Combust. and Flame 107, 418–452 (1996).
18. Vander Wal, R.L., Zhou, Z., and Choi, M.Y., Combust. and Flame 105, 462–470 (1996).
19. Will, S., Schraml, S., and Leipertz, A., Twenty-Sixth Symposium (International) on Combustion, The Combustion Institute, Pittsburgh, PA, p. 2277 (1996).
20. Vander Wal, R.L., Ticich, T.M., and Stephens, A.B., Comb. and Flame 116, 291–296 (1999).
21. Vander Wal, R.L., Appl. Optics 35, 6548–6559 (1996).
22. Vander Wal, R.L. and Jensen, K.A., Appl. Opt. 37, 1607–1616 (1998).
23. Vander Wal, R.L., Ticich, T.M., and Stephens, A.B., Appl Phys. B67, 115–123 (1998).
24. Filippov, A.V., Markus, M.W., and Roth, P., J. Aerosol Sci. 30, 71–87 (1999).
25. Filippov, A.V., Rosner, D.E., and Kumar, M., Abstract presented at The Joint Meeting of the United States Sections: The Combustion Institute, March 15–17 (1999).
26. Vander Wal, R.L., Ticich, T.M., and West, J.R. Jr., Appl. Opt. (in press).

REPORT DOCUMENTATION PAGE

Form Approved
OMB No. 0704-0188

1. AGENCY USE ONLY (*Leave blank*)	2. REPORT DATE	3. REPORT TYPE AND DATES COVERED
	February 2000	Final Contractor Report

4. TITLE AND SUBTITLE

Development and Characterization of Laser-Induced Incandescence Towards Nanoparticle (Soot) Detection

5. FUNDING NUMBERS

WU–963–70–0P–00
NAS3–544

6. AUTHOR(S)

Randy L. Vander Wal

7. PERFORMING ORGANIZATION NAME(S) AND ADDRESS(ES)

National Center for Microgravity Research
John H. Glenn Research Center at Lewis Field
Cleveland, Ohio 44135–3191

8. PERFORMING ORGANIZATION REPORT NUMBER

E–11854

9. SPONSORING/MONITORING AGENCY NAME(S) AND ADDRESS(ES)

National Aeronautics and Space Administration
John H. Glenn Research Center at Lewis Field
Cleveland, Ohio 44135–3191

10. SPONSORING/MONITORING AGENCY REPORT NUMBER

NASA CR—2000-209309

11. SUPPLEMENTARY NOTES

Prepared for the Symposium on Nanoparticles cosponsored by the National Science Foundation and the European Science Foundation, Tacoma, Washington, October 10, 1999. Project Manager, Steve Simons, Microgravity Science Division, NASA Glenn Research Center, organization code 6700, (216) 433–5277.

12a. DISTRIBUTION/AVAILABILITY STATEMENT

Unclassified - Unlimited
Subject Categories: 23 and 45 Distribution: Nonstandard

This publication is available from the NASA Center for AeroSpace Information, (301) 621–0390.

12b. DISTRIBUTION CODE

13. ABSTRACT ***(Maximum 200 words)***

The production of particulates, notably soot, during combustion has both positive and negative ramifications. Exhaust from diesel engines under load (for example, shifting gears), flickering candle flames and fireplaces all produce soot leaving a flame. From an efficiency standpoint, emission of soot from engines, furnaces or even a simple flickering candle flame represents a loss of useful energy. The emission of soot from diesel engines, furnaces, power generation facilities, incinerators and even simple flames poses a serious environmental problem and health risk. Yet some industries intentionally produce soot as carbon black for use in inks, copier toner, tires and as pigments. Similarly, the presence of soot within flames can act both positively and negatively. Energy transfer from a combustion process is greatly facilitated by the radiative heat transfer from soot yet radiative heat transfer also facilitates the spread of unwanted fires. To understand soot formation and develop control strategies for soot emission/formation, measurements of soot concentration in both practical devices such as engines and controlled laboratory flames are necessary. Laser-induced incandescence (LII) has been developed and characterized to address this need, as described here.

14. SUBJECT TERMS

Nanoparticles; Particle; Soot; Detection

15. NUMBER OF PAGES

18

16. PRICE CODE

A03

17. SECURITY CLASSIFICATION OF REPORT	18. SECURITY CLASSIFICATION OF THIS PAGE	19. SECURITY CLASSIFICATION OF ABSTRACT	20. LIMITATION OF ABSTRACT
Unclassified	Unclassified	Unclassified	